

Detection of a molecular hydrogen envelope around nova GK Persei

D. P. K. BANERJEE ¹, A. EVANS ², T. LIIMETS ³, C. E. WOODWARD ⁴, T. R. GEBALLE ⁵, V. JOSHI ⁶
AND S. STARRFIELD ⁷

¹*Astronomy and Astrophysics Division, Physical Research Laboratory, Ahmedabad, India 380009*

²*Astrophysics Research Centre, Lennard Jones Laboratories, Keele University, Keele, Staffordshire ST5 5BG, UK*

³*Tartu Observatory, University of Tartu, Observatooriumi 1, Toravere 61602, Estonia*

⁴*Minnesota Institute for Astrophysics, School of Physics & Astronomy, 116 Church Street SE, University of Minnesota, Minneapolis, MN 55455, USA*

⁵*Gemini Observatory/NSF's NOIRLab, 670 N. Aohoku Place, Hilo, HI, 96720, USA*

⁶*Physical Research Laboratory, Navrangpura, Ahmedabad, Gujarat 380009, India*

⁷*School of Earth and Space Exploration, Arizona State University, Box 876004, Tempe, AZ 85287-6004, USA*

(Received 2026 February 15; Accepted 2026 March 12)

ABSTRACT

The eruption of Nova Persei 1901 (GK Per) occurred 125 yrs ago; remarkably it still holds major surprises. Using data from the Spectro-Photometer for the History of the Universe, Epoch of Reionization, and Ices Explorer (SPHEREx), we find it has a bipolar molecular hydrogen shell. This shell, which has dimensions $18' \times 10'$, is co-spatial with the H α nebulosity surrounding the nova, which is purported to be an ancient planetary nebula (PN). The shell is detected most strongly in the 0–0 $S(9)$ 4.6947 μm line. A filament of emission in the $S(9)$ 4.6947 μm line is seen $\simeq 45''$ South-West of GK Per. This coincides, over much of its length, with the site of X-ray and non-thermal radio emission where the 1901 nova ejecta impinges on the ambient medium. We propose that the H₂ emission from the filament arises from the predicted neutral zone between the forward and reverse shocks. Since it is common for bipolar PNe to be accompanied by H₂ envelopes, it ostensibly suggests that the $18' \times 10'$ nebulosity is a conventional PN with a luminous, ionizing central source. We show this is not the case, and that the H α nebulosity may be surrounding gas belonging to pre-existing material that was ionized during the 1901 eruption. The ionized gas is presently undergoing recombination on a timescale of $\simeq 3000$ years, explaining why the nebulosity is still visible.

Keywords: Classical novae(251) — Circumstellar matter(241)

1. INTRODUCTION

Nova Persei 1901 (GK Per) was the first bright classical nova of the 20th century. Seven months after eruption, superluminal light echoes were detected (G. W. Ritchey 1901a,b, 1902); however ejecta from the nova outburst became visible only 15 years later (F. A. P. Barnard 1916). Since then, the remnant of the 1901 outburst has been extensively studied (e.g., E. R. Seaquist et al. 1989; G. C. Anupama & T. P. Prabhu 1993; T. Liimets et al. 2012; E. Harvey et al. 2016, and references therein). It has a round, overall morphology consisting of almost a thousand cometary-like structures, as revealed by high-resolution images from the Hubble Space Telescope (M. M. Shara et al. 2012), and currently extends to a radius of $\sim 1'$. The expansion velocities

of individual knots in the remnant have been measured to mostly lie between 600 and 1000 km s^{-1} by T. Liimets et al. (2012), who found that the remnant is best described as a thick spherical shell. E. Harvey et al. (2016), using the same data, proposed an equally satisfactory alternative model, consisting of an equatorial barrel feature with polar cones.

A considerably larger ($\sim 20'$) bipolar structure, compared to the nova remnant, was discovered at 60 μm and 100 μm in Infrared Astronomical Satellite (IRAS, G. Neugebauer et al. 1984) data by M. F. Bode et al. (1987), who proposed an ancient planetary nebula (PN) origin. This interpretation was based on several arguments: (a) the bipolar, toroidal morphology of the structure; (b) its symmetric centering on the central star; (c) the large inferred total mass, which they argued is more consistent with a PN than with a nova remnant; (d) the absence of a significant temperature gradient across the nebula; and (e) kinematic measurements sug-

gesting expansion velocities of only a few km s^{-1} , implying a timescale compatible with a PN origin. They excluded the possibility that the structure represents swept-up interstellar material produced by the nova outburst, arguing that the nova shock would neither be energetic enough nor capable of generating such a large-scale structure. In particular, they noted that the H I line width shows little evidence for velocities exceeding $\sim 5 \text{ km s}^{-1}$ (E. R. Seaquist et al. 1989).

E. R. Seaquist et al. (1989) describe H I emission of the region, which has a morphology similar to the IRAS dust nebula. Their main conclusion was that, while it is plausible that the bipolar structure is a PN, there are several issues with this interpretation: (a) asymmetry in the nova or/and PN outburst is required; (b) the estimated age of $\sim 100\,000$ years for the PN, which taking into account the theory of the isolated cooling white dwarf (WD), would require a higher luminosity for the WD primary than is observed in the case of GK Per; (c) the complex structure of the interstellar medium around GK Per compared to the features in the IRAS and H I images, so that it is inconclusive whether or not their origin is circumstellar.

F. V. Hessman (1989) presented ^{12}CO observations of the same region, and concluded that at least part of this emission originates from interstellar cirrus, suggesting that the large-scale environment around GK Per likely includes a contribution from unrelated interstellar material in addition to any circumstellar component. They argue that, while the ^{12}CO emission in the southeast (SE) lobe correlates well with the far-infrared emission, it is completely absent from the northwest (NW) side. The estimated ^{12}CO mass ($2 M_{\odot}$) is inconsistent with that expected from formation of a PN due to mass loss from the progenitor star (e.g., P. Ventura et al. 2025). Furthermore, the ^{12}CO velocities were no greater than a few km s^{-1} .

A. D. Scott et al. (1994) reported a high-spatial-resolution study of the immediate environment of GK Per in the $J = 2 - 1$ transition of ^{12}CO . Their observations revealed an apparent bipolar emission structure centered on the nova, with lobes expanding symmetrically at velocities of approximately $2.0\text{--}4.5 \text{ km s}^{-1}$, comparable to those measured by E. R. Seaquist et al. (1989). The morphology of the CO emission broadly resembles the bipolar structure seen in the IRAS data. However, the detected features are located near the edge of the field of view, indicating that the CO nebula likely extends beyond the mapped area. Based on the observed velocity field, they favored an interpretation in terms of bipolar lobes rather than a toroidal geometry. The inferred dimensions, expansion velocities, and total mass of the molecular nebula are consistent with those of PNe, with an estimated total hydrogen mass of $\sim 0.05 M_{\odot}$, and an age of $\sim 2.4 \times 10^5$ yr. On this basis, they concluded that GK Per is surrounded by a fossil PN rather than a coincidental interstellar matter. However the ob-

servations of T. Kamiński et al. (2022) cast doubt on this conclusion. These authors analyzed archival Wide-field Infrared Explorer (WISE, H. R. Schember et al. 1996) data in conjunction with new, more extended, CO observations in the $J = 1 - 0$ and $J = 2 - 1$ transitions. They concluded that, while the CO emission is most probably interstellar, the emission in WISE and in the optical range is most probably circumstellar.

The H α counterpart of the structure was discovered by R. W. Tweedy (1995). It shows the same bipolar morphology, but with a dominant ridge in the southwest (SW) that is not seen in the IRAS data. However, it corresponds to the region containing the brightest light echoes detected between 1901 and 1902 (G. W. Ritchey 1901a,b, 1902). R. W. Tweedy (1995) argued against a PN interpretation, noting that the temperature and inferred evolutionary state of the WD are inconsistent with the age required for a PN of this size. Instead, they proposed scenarios in which the nebula consists of accumulated material from (i) multiple previous nova eruptions or (ii) sustained mass loss during extended quiescent phases. This interpretation has credence as the nebula was already present at the time of the light echoes, implying a long-lived structure formed through repeated or prolonged mass ejection rather than a single event. On the other hand, S. M. Dougherty et al. (1996) argue that the extended emission is physically related to the central binary, based on the symmetric morphology seen in the IRAS data. However, they assert that a more plausible explanation is that the secondary star evolved off the main sequence and expanded, leading to a phase of enhanced mass transfer onto the WD. This triggered a brief born-again asymptotic giant branch-like phase, accompanied by substantial mass loss, giving rise to the extended bipolar nebulosity.

All of the above studies, including also the analysis by M. F. Bode et al. (2004), demonstrate the extensive debate, and many questions relating to the nature of GK Per. In this paper we present wide field low resolution infrared spectral imagery recently obtained by the Spectro-Photometer for the History of the Universe, Epoch of Reionization, and Ices Explorer (SPHEREx, B. P. Crill et al. 2020; J. J. Bock et al. 2025, and details therein) in order to address some of these questions.

For comparison with the SPHEREx data, we utilize a previously unpublished optical image of the GK Per region, shown in Figure 1. The wide field of view is needed in order to compare the morphology and characteristics of the putative PN in the optical with those in the infrared.

2. OBSERVATIONS AND RESULTS

SPHEREx is a NASA space telescope that produces an all-sky map in 102 color bands covering the range $0.75\text{--}5.0 \mu\text{m}$. It contains six linear Variable Filters (LVFs) arranged over six HgCdTe detector arrays and



Figure 1. The top panel shows a deep image of GK Per and its surroundings obtained by the Deep Sky Collective (DSC^a). The total exposure time was 265h 50m. Images were obtained in various filters. The per-filter exposure times were 13h 00m (Lum/clear), 14h 20m (R), 16h 15m (G), 15h 45m (B), 91h 55m ([O III], 5 nm bandpass), 14h 35m (H α , 5 nm bandpass). For the color palette, the broadband is RGB with luminance being used for details and signal (the infrared cirrus hence appears grey). H α is red and [O III] is mapped to R and G, giving it a cyan-blueish look. The field of view is 50' \times 43'. North is up, and East is to the left. The bottom panel shows contours at surface brightness levels of 0.72, 1.05 and 1.20 MJy/sr in the 4.6947 μ m H $_2$ emission line (discussed in Section 2) observed by SPHEREx superposed on the optical image.

^a<https://ssr.app.astrobin.com/i/ocm8rv?r=0>

thus sequentially collects data in six wavelength bands, whose characteristics are summarized in Table 1.

SPHEREx obtained 114 spectrophotometric images of GK Per and its environs, covering all 102 of its wavelength bands. The exposure time for each image was 113.58 s. Emission was detected in \sim 30 of the images. Because of the low spectral resolution (see Table 1), precise wavelengths of each emission feature cannot be determined from the spectra. However, the wavelengths of each of the bands in which emission was detected encom-

pass sets of lines of the $v=1-0$ band and pure rotational ($v=0-0$) band of molecular hydrogen (H $_2$). All of these detections are self-consistent with this identification, in the sense that all of these lines of H $_2$ might be reasonably expected to be present if some are present. The detected lines, numbering about 30 are listed in Table 1. A few of the detections are blends of H $_2$ lines of different intrinsic strengths at nearby wavelengths that are not resolved by SPHEREx. Due to the weakness of the H $_2$ emission and thus the low signal-to-noise ratios on all but the strongest lines, not all of the lines in Table 1 are clearly detected in all 30 of the images at all locations in GK Per where the stronger lines are detected. However, they are present in a sufficient number of locations that we regard all of these individual lines and blends as real detections, rather than artifacts. To our knowledge, these observations constitute the first detection of H $_2$ in GK Per.

Images of the 1-0 $S(1)$ 2.1218 μ m, the combined 2-1 $S(1)$ 2.2477 μ m and 1-0 $S(0)$ 2.2235 μ m, the 1-0 $Q(1)$ 2.4066 μ m, and the 0-0 $S(9)$ 4.6947 μ m lines are shown in Figure 2. As can be seen by comparing these images with Figure 1, emission regions in the three brightest lines have the same orientation on the sky as the H α emission, have similar dimensions (18' \times 10') as the H α emission, and, like it, are strongest at the edges of the region.

We have extracted spectra at several locations in the nebula using the spectrophotometry tool available at the SPHEREx website¹. Several 4 to 5 μ m segments of these spectra are presented in Figure 3, along with one spectrum covering the entire wavelength range. Each of the 4-5 μ m spectra shows emission in the 0-0 $S(9)$ line. As can be seen in central panel of the figure, that line is present over nearly the entire 18' \times 10' nebula. The 0-0 $S(10)$ 4.4096 μ m line is also present in most of these spectra, since emission is present in its color band.

In general, the intensity ratios of H $_2$ lines allow one to determine H $_2$ temperature and distinguish between excitation mechanisms for the molecule, in particular between collisional (e.g., shock) excitation and UV excitation. However, the inherent process by which SPHEREx data are recorded does not allow one to compare line strengths directly to use as diagnostics. Wavelength scanning in SPHEREx is done by nodding the telescope several times in the north-south direction, so that a star lies on different positions of the LVF (and hence at different wavelengths). Thus, for an extended source (such as the GK Per nebula), there is a vertical wavelength gradient between its north and south tips. Hence comparing the peak intensities of two lines from the same location on the nebula cannot be done directly because at that position the two lines could be shifted by different amounts from their corresponding rest wavelengths.

¹ <https://www.jpl.nasa.gov/missions/spherex/>

Nevertheless, some basic conclusions can be reached. Both the large range of rotational levels that are populated in the $v = 0$ state, and the high intensity of the 0–0 $S(9)$ line relative to the other pure rotational lines indicate collisions are the dominant excitation mechanism. This conclusion is supported by the obviously very low intensity ratio of the combined 1–0 $S(0)$ and 2–1 $S(1)$ lines at $2.224 \mu\text{m}$ and $2.248 \mu\text{m}$, respectively, to that of the 1–0 $S(1)$ line at $2.122 \mu\text{m}$, apparent from the examination of panels A and B in Figure 2. Historically, the ratio of these two lines is the most common way of distinguishing between collisional and UV excitation as discussed in J. H. Black & E. F. van Dishoeck (1987, see Figure 2) or I. Gatley et al. (1987).

Going beyond this basic level of analysis of relative line intensities is highly problematic. For example, in Figure 3 the full spectrum at Position 1 is totally dominated by the 0–0 $S(9)$ line; all other lines appear weaker than it by at least an order of magnitude. We believe there is no reasonable physical explanation for this. Very high extinction by dust could account for some of the anomaly, but not all of it and, in addition, no evidence for high extinction by dust exists. Moreover, the nearby $S(10)$ $4.4096 \mu\text{m}$ line, which should be roughly one-third the strength of the $S(9)$ line (as the ratio of ortho-to-para hydrogen is generally 3:1 in statistical equilibrium) and should suffer nearly the same extinction by dust, is not detected. We conclude that determination of line strengths requires a level of data analysis beyond the scope of this paper, as well as a better understanding by us of the details of the performance of SPHEREx.

A faint arc of emission is evident in the $4.69947 \mu\text{m}$ image containing the H_2 0–0 $S(9)$ line, which coincides well with the SW edge of the nova ejecta. This may be seen by overlaying a $\text{H}\alpha$ image taken by us in 2023 October with the Isaac Newton Telescope (see Figure 2). The H_2 arc also coincides, over a large part, with the intense X-ray arc (§. Balman 2005) and with the radio arc from synchrotron emission (E. R. Seaquist et al. 1989; A. J. Slavin et al. 1995) found at the same position. A composite optical/radio/X-ray picture showing this arc is available at <https://chandra.harvard.edu/photo/2015/gkper/>. Likely this arc is cool H_2 -bearing material between the forward and reverse shock as the nova ejecta encountered the ambient medium. The presence of such cool material was argued for by §. Balman (2005), based on the greater neutral H absorption seen in the X-ray component associated with the reverse shock vis-a-vis a lesser neutral H absorption in the forward shock. This additional absorption indicated a neutral H zone lay between the shocks (§. Balman 2005). Theoretically, such a zone between the forward and reverse shocks is predicted, both in novae and supernovae, as their ejecta propagate into their surrounding medium (e.g., C. Fransson et al. 1996; A. M. Derdzinski et al. 2017). This cool zone is precisely where molecules and dust are proposed to form (A. M. Derdzinski et al. 2017),

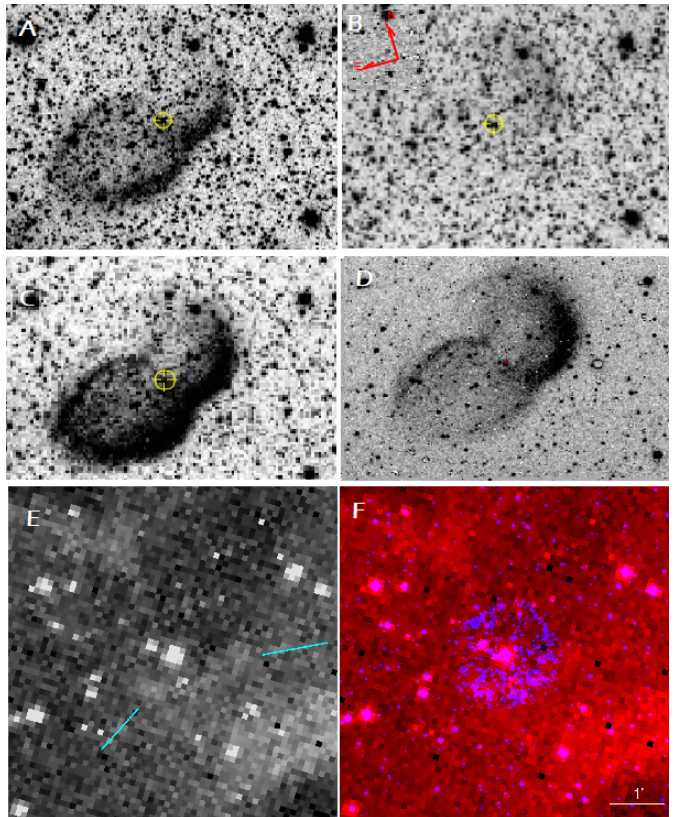


Figure 2. SPHEREx images of GK Per in the 1–0 $S(1)$ $2.1218\mu\text{m}$ (panel A), the combined 1–0 $S(0)$ $2.2235 \mu\text{m}$ and 2–1 $S(1)$ $2.2477 \mu\text{m}$ (panel B), 1–0 $Q(1)$ $2.4066 \mu\text{m}$ (panel C) and 0–0 $S(9)$ $4.6947 \mu\text{m}$ lines (panel D). The first three afore-mentioned images are presented with the same color and stretch settings. Panels A through D have a field of view $\approx 24'.0 \times 18'.5$. The weakness of the combined 1–0 $S(0)$ and 2–1 $S(1)$ lines compared to that of 1–0 $S(1)$ ($2.1218 \mu\text{m}$), indicates that shock excitation rather than UV-fluorescence is the excitation mechanism (see text). The $4.6947 \mu\text{m}$ image (middle right) shows a filament of H_2 emission about $44''$ south-west ($\text{PA} = 145^\circ$) of the central star. This filament is magnified in panel E (North to the top) and shown between markers in cyan. Overlaid on this image, but now shown in red in panel F, is an $\text{H}\alpha$ image taken by us in 2023 showing the nova ejecta of 1901 in blue. The SW rim of the nova ejecta coincides with the filament over a large extent. The position of the filament was the site of intense X-ray and non-thermal radio emission. The size scale of $1'.0$ valid for panel E and F only is inset in the lower right of panel F.

so the presence of H_2 in the arc is consistent. This result is a rare synthesis of theory, and optical, radio, X-ray, and infrared observations.

3. DISCUSSION

The discovery of the H_2 envelope around GK Per may favor the classification of its large nebulosity as a PN. PNe, and bipolar PNe specifically, are often known to

Table 1. Observational details and list of detected lines

SPHEREX	λ	R^a	SPHEREx	Date	H ₂	λ (vac)	E_2
band	range (μm)		ID	MJD	line	(μm)	(K) ^b
D6	4.42–5.00	128	2025W35_1A_0217_2	60913.035283	0–0 $S(10)$	4.4096	11940
"			2025W35_1A_0518_2	60914.664914	0–0 $S(9)$	4.6947	10263
"			2025W35_1A_0518_3	60914.666407	0–0 $S(9)$	4.6947	10263
D5	3.82–4.42	112	2025W34_1B_0174_3	60905.904597	0–0 $S(11)$	4.1810	13703
"			2025W34_1B_0174_4	60905.906090	0–0 $S(10)$	4.4096	11940
"			2025W34_1B_0187_2	60905.971393	0–0 $S(10)$	4.4096	11940
"			2025W33_1B_0598_4	60911.679808	0–0 $S(12)$	3.9947	15549
"			2025W33_1B_0393_2	60910.589958	0–0 $S(13)$	3.8464	17458
"			2025W33_1B_0393_3	60910.591468	0–0 $S(13)$	3.8464	17458
"			2025W33_1B_0598_2	60911.676816	0–0 $S(13)$	3.8464	17458
D4	2.42–3.82	35	2025W34_1B_0035_2	60905.152963	1–0 $O(7)$	3.8075	8365
"			2025W34_1B_0102_1	60905.492522	1–0 $O(6)$	3.5007	7485
"			2025W34_1B_0102_1	60905.492509	1–0 $O(6)$	3.5007	7485
"			2025W34_1B_0048_2	60905.2219708	1–0 $O(5)$	3.2350	6956
"			2025W34_1B_0048_1	60905.220416	1–0 $O(4)$	3.0039	6471
"			2025W34_1B_0062_1	60905.289948	1–0 $O(4)$	3.0039	6471
"			2025W34_1B_0048_2	60905.221908	1–0 $O(5)$	3.2350	6956
"			2025W34_1B_0062_1	60905.289916	1–0 $O(4)$	3.0039	6471
"			2025W33_2C_0028_2	60901.619552	1–0 $O(4)$	3.0039	6471
"			2025W33_2C_0014_3	60901.554479	1–0 $O(3)$	2.8025	6149
"			2025W33_2C_0014_4	60901.555972	1–0 $O(3)$	2.8025	6149
"			2025W33_2C_0014_1	60901.551506	1–0 $O(2)$	2.6269	5987
"			2025W33_2C_0014_2	60901.552987	1–0 $O(2)$	2.6269	5987
"			2025W33_1B_0652_4	60901.488465	1–0 $Q(7)$	2.5001	10341
"			2025W33_1B_0652_3	60901.488465	1–0 $Q(6)$	2.4756	9286
"			2025W33_1B_0652_3	60901.488465	1–0 $Q(4)$ to $Q(7)$	2.4548	8365
"			2025W33_1B_0652_2	60901.486973	1–0 $Q(1)$ to $Q(4)$	2.4375	7586
D3	1.64–2.42	41	2025W34_2B_0490_2	60911.134133	1–0 $Q(1)$ to $Q(4)$	2.4066	6149
"			2025W34_2B_0443_4	60910.864888	1–0 $S(0)$	2.2235	6471
"			2025W35_1A_0187_1	60912.897232	1–0 $S(0)$	2.2235	6471
"			2025W34_2B_0443_3	60910.863395	1–0 $S(1)$	2.1218	6956
"			2025W34_2B_0304_1	60910.113145	1–0 $S(2)$	2.0338	7584
"			2025W34_2B_0443_1	60910.860411	1–0 $S(2)$	2.0338	7584
"			2025W34_2B_0443_2	60910.861903	1–0 $S(1)$	2.0338	6956
"			2025W35_1A_0518_3	60914.666407	1–0 $S(2)$, $S(3)$	2.0338	7584
"			2025W37_2A_0034_1	60929.610165	1–0 $S(2)$	2.0338	7584
"			2025W35_1A_0518_2	60914.664914	1–0 $S(3)$	1.9576	8365
"			2025W35_1A_0518_1	60914.663422	1–0 $S(4)$	1.8920	9286
"			2025W35_1A_0441_4	60914.260211	1–0 $S(5)$	1.8358	10341
"			2025W35_1A_0441_3	60914.258719	1–0 $S(6)$	1.7880	11522
"			2025W35_1A_0441_1	60914.255735	1–0 $S(7)$, $S(8)$	1.7480	12817
"			2025W35_1A_0441_2	60914.257227	1–0 $S(7)$	1.7480	11522

NOTE—^aResolution $R = \lambda/\Delta\lambda$. ^bEnergy of upper level. All observations were 113.58 sec. The SPHEREx IDs were taken from the IRSA/IPAC site

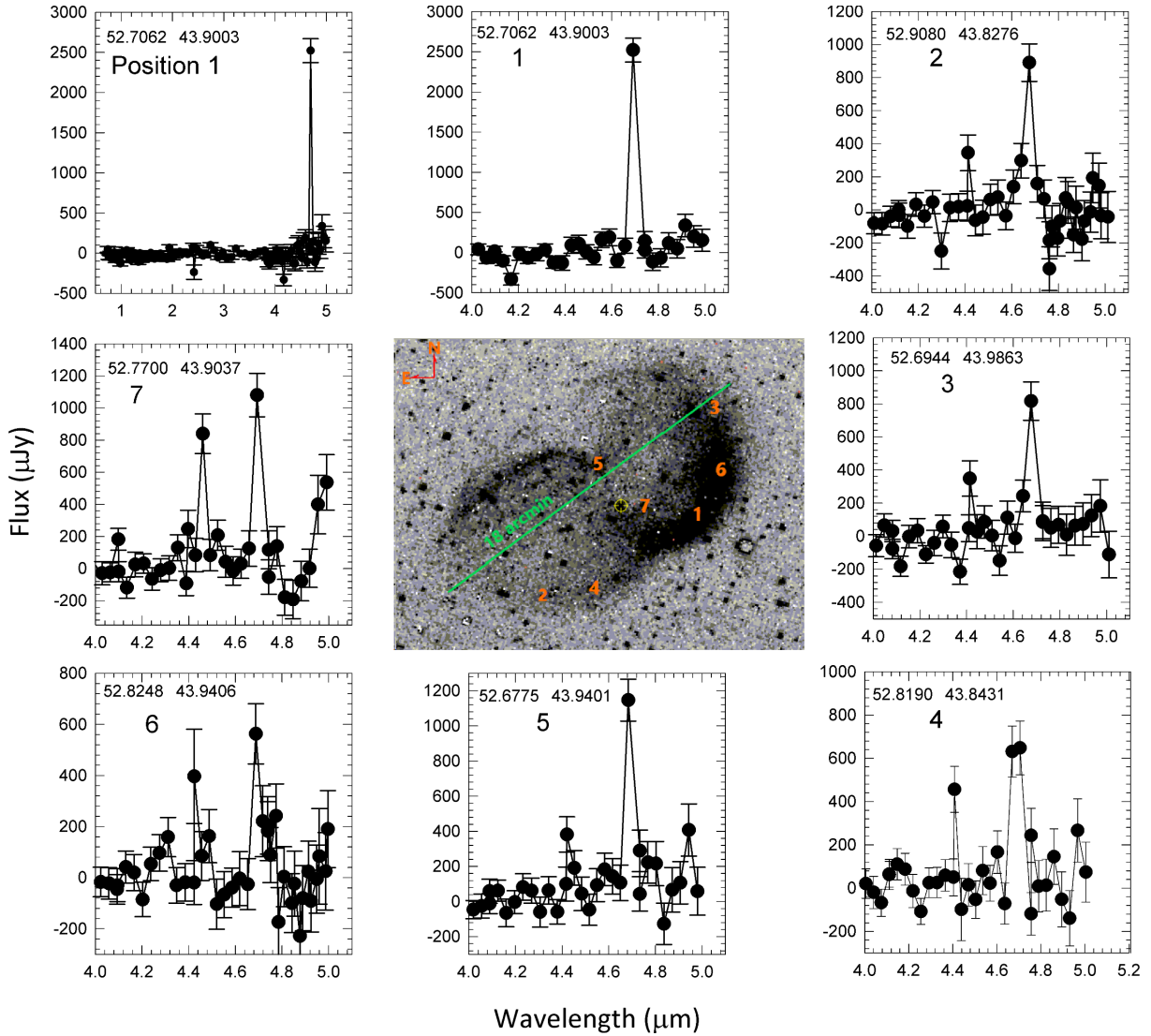


Figure 3. SPHEREx spectra at selected positions on GK Per whose image in the H_2 0–0 $S(9)$ $4.6947 \mu\text{m}$ line is shown at center. Markers on the image indicate positions where spectra are shown here and whose spatial location on the nebula and corresponding RA and Dec (2000) positions (in degrees) are indicated at the top left in each panel. The top left panel shows a representative spectrum covering the entire $0.75\text{--}5 \mu\text{m}$ region measured at position 1; the rest of the spectra focus on the region covering the 0–0 $S(9)$ $4.6947 \mu\text{m}$ line which was the strongest line in the spectrum and which is seen at almost all the positions. More details are given in the text (Section 3.) The upward rise of some the spectra near $5.0 \mu\text{m}$ is likely due to the 0–0 $S(8)$ $5.0529 \mu\text{m}$ line.

have such H₂ shells (J. H. Kastner et al. 1996; A. K. Speck et al. 2003; G. Ramos-Larios et al. 2017). For GK Per, the mass of the putative PN, based on the H α nebulosity seen in Figure 1, can be estimated by assuming the two-dimensional 18' \times 10' PN to be approximately an ellipsoid in three dimensions with semi-major axes $a, b, c = 9', 5', 5'$. For an assumed distance of 470 pc, assuming that its hydrogen is fully ionized and that the electron density $n_e = 40 \text{ cm}^{-3}$ (this value is justified below), the mass lies in the range 0.28–0.38 M $_{\odot}$, assuming a mean value of the filling factor between 0.3 to 0.4 (F. R. Boffi & L. Stanghellini 1994). This is consistent with the range of PNe masses, 0.1–1.0 M $_{\odot}$ (J. P. Phillips & S. R. Pottasch 1984).

However, there are a few inconsistencies with the PN scenario. A bipolar shape invariably needs a dense equatorial constriction (e.g., a torus) to shape the nebula, but clear evidence for such a torus is not seen in the images here. Such a torus or equatorial constriction is expected to be dense and hence the likely site of H₂ and dust (e.g., the hourglass nebula NGC 2346; I. Gatley & B. Zuckerman 1986; G. Ramos-Larios et al. 2017). The velocity kinematics across the field also appear to be on the lower side, from the limited radio studies (see Section 1), compared to typical PNe expansion velocities V_{exp} of 10–30 km s⁻¹, although very old PNe can have lower V_{exp} values (T. J. Bohuski & M. G. Smith 1974). Observational tests for the bipolarity of the nebula can be done by measurements of V_{exp} at the waist and poles. Bipolar flows generally follow a $V \propto r$ law (homologous flow) and thus the waist expands much more slowly than the poles.

Other arguments against a PN interpretation arise from the timescales involved in the evolution of a 0.82 and a 1.0 M $_{\odot}$ star (e.g., M. M. Miller Bertolami 2016). These tracks were selected because the WD in GK Per has a mass between $\simeq 0.8$ to 1.0 M $_{\odot}$ (D. Crampton et al. 1986; L. Morales-Rueda et al. 2002; A. Álvarez-Hernández et al. 2021). From these tracks we note, that taking 30,000 K as the lower end of the temperature range for the central stars of PNe (CSPNe), PN should form within a few years. The tracks also indicate that the time to reach WD luminosities of 10^{-2} to 10^{-3} L $_{\odot}$ at which conventional nova models are generated (J. José & M. Hernanz 1998; S. Starrfield et al. 2024, 2025) is more than a million years. Since the general lifespan of a PN is between $\simeq 10,000$ to 30,000 yrs, the PN would have faded below detection level by the time the nova erupted in 1901. Hence, it should not be possible to see the PN and the nova remnant at the same time. Further, the mass of the present WD in GK Per is higher than the known mass of any CSPN, irrespective of whether the CSPN is a single star or is in a binary system (see Figure 13 of W. A. Weidmann et al. 2020, for a histogram of CSPNE masses). The model WD luminosities used, between 10^{-2} to 10^{-3} L $_{\odot}$ that are needed to initiate and drive the nova eruption, could not have been that of a

CSPN because there are no observed CSPNe with luminosities $\lesssim 1$ L $_{\odot}$. We have determined this by plotting the archival data within Figure 5 (histogram of CSPNe luminosities) in W. A. Weidmann et al. (2020). From all these arguments the nebulosity cannot be a conventional PN.

We have also considered whether the PN could be a nova super-remnant (NSR) created by repeated eruptions of a recurrent nova sweeping out the circumstellar material. NSR's were first discovered around M31N 2008-12a (M. J. Darnley et al. 2019) and subsequently around the Galactic RNe KT Eridani (M. M. Shara et al. 2024a; M. W. Healy-Kalesh et al. 2024), T CrB (M. M. Shara et al. 2024b) and RS Ophiuchi (M. M. Shara et al. 2025). However, these NSRs have diameters ranging from ~ 30 to 130 pc whereas the H α nebulosity here is much smaller. Based on its angular size, the semi-minor and major axes are ~ 0.7 and 1.2 pc respectively.

Thus, as an alternative to the PN scenario, we consider whether the nebulosity is actually material that pre-existed the 1901 eruption of GK Per, which was thereafter ionized by the nova outburst and is presently in the recombination phase. There is substantial material around GK Per, as evidenced in HI and CO mapping studies, IRAS and WISE imagery, and the detection of a light echo (Section 1). The H α gas in the nebulosity is certainly at low density, because imaging of the jet by M. M. Shara et al. (2012, see their Figure 12) also showed parts of the nebulosity emitting in H α , and it is clearly seen that the surface brightness of the jet is substantially greater than that of the PN nebulosity. Since the density of the jet was estimated to be 20–40 cm⁻³ from the [S II] lines (M. M. Shara et al. 2012), assuming $n_e = 40 \text{ cm}^{-3}$ as the upper limit for the nebulosity is justified. The Case B recombination time for ionized hydrogen with density n_e and temperature T_e is $(\alpha(T_e)n_e)^{-1}$. Here, the recombination rate coefficient $\alpha(T_e) = 2.6 \times 10^{-13} \text{ cm}^3 \text{ s}^{-1}$ for an assumed $T_e = 10000 \text{ K}$ under Case B conditions. The recombination time is hence ~ 3000 years, and could explain why the nebulosity remains visible today.

An apparent inconsistency in this scenario is that the secondary, if evolving as a single star, would take $\gtrsim 1$ Gyr to evolve to its present K2 IV state. In contrast, a 0.9 M $_{\odot}$ WD would take $(5-8) \times 10^7$ yr to evolve from the main-sequence to the WD stage (S. M. Dougherty et al. 1996). This mismatch between time scales can possibly be resolved if there has been mass exchanges between the two components in the past, through Roche Lobe overflow (S. M. Dougherty et al. 1996). This may explain why the K type secondary, whose mass has variously been estimated between 0.25 to 0.48 M $_{\odot}$ is under massive for its spectral type (D. Crampton et al. 1986; A. Álvarez-Hernández et al. 2021). Similar systems do exist, such as UCAC2 46706450 which has a WD with a K subgiant secondary (K. Werner et al. 2020). Furthermore, surveys of S. G. Parsons et al. (2016) have

established a large group of main sequence FGK stars which show excess UV flux, and hence likely have a WD companions (K. Werner et al. 2020).

GK Per and its environment remain partially understood and the more we discover about it, the more we realize how incomplete is our understanding of it. There is a need for a spatio-kinematic study of the nebulosity to further test its classification as a PN, and thence understand its relation to the 1901 outburst.

Facilities: SPHEREx, INT:Newton

ACKNOWLEDGMENTS

The authors thank the referee for their insightful and thoughtful comments that improved the manuscript. This publication makes use of data products from the Spectro-Photometer for the History of the Universe, Epoch of Reionization and Ices Explorer (SPHEREx),

which is a joint project of the Jet Propulsion Laboratory and the California Institute of Technology, and is funded by the National Aeronautics and Space Administration. SPHEREx data used in this manuscript can be found at 10.26131/IRSA629 SPHEREx Quick Release Spectral Images, <https://doi.org/10.26131/IRSA629>. We thank the many amateur astronomers who contributed to the striking Deep Sky Collective² image, and Tim Schaeffer for permission to reproduce it here. We thank Marcelo Miller Bertolami for kindly providing the evolutionary tracks for the 1 M_{\odot} star. SS acknowledges partial support from a NASA Emerging Worlds grant to ASU (80NSSC22K0361) as well as support from his ASU Regents' Professorship and JWST/NASA. CEW acknowledges partial support from NASA JWST-06866.022-A. VJ and DPKB acknowledge support from PRL, Ahmedabad and the Department of Space, Government of India.

REFERENCES

- Álvarez-Hernández, A., Torres, M. A. P., Rodríguez-Gil, P., et al. 2021, MNRAS, 507, 5805, doi: [10.1093/mnras/stab2547](https://doi.org/10.1093/mnras/stab2547)
- Anupama, G. C., & Prabhu, T. P. 1993, MNRAS, 263, 335, doi: [10.1093/mnras/263.2.335](https://doi.org/10.1093/mnras/263.2.335)
- Balman, Ş. 2005, ApJ, 627, 933, doi: [10.1086/430392](https://doi.org/10.1086/430392)
- Barnard, F. A. P. 1916, Harvard College Observatory Bulletin, 621, 1
- Black, J. H., & van Dishoeck, E. F. 1987, ApJ, 322, 412, doi: [10.1086/165740](https://doi.org/10.1086/165740)
- Bock, J. J., Aboobaker, A. M., Adamo, J., et al. 2025, arXiv e-prints, arXiv:2511.02985, doi: [10.48550/arXiv.2511.02985](https://doi.org/10.48550/arXiv.2511.02985)
- Bode, M. F., O'Brien, T. J., & Simpson, M. 2004, ApJL, 600, L63, doi: [10.1086/381529](https://doi.org/10.1086/381529)
- Bode, M. F., Seaquist, E. R., Frail, D. A., et al. 1987, Nature, 329, 519, doi: [10.1038/329519a0](https://doi.org/10.1038/329519a0)
- Boffi, F. R., & Stanghellini, L. 1994, A&A, 284, 248, doi: [10.48550/arXiv.astro-ph/9310037](https://doi.org/10.48550/arXiv.astro-ph/9310037)
- Bohuski, T. J., & Smith, M. G. 1974, ApJ, 193, 197, doi: [10.1086/153147](https://doi.org/10.1086/153147)
- Crampton, D., Cowley, A. P., & Fisher, W. A. 1986, ApJ, 300, 788, doi: [10.1086/163856](https://doi.org/10.1086/163856)
- Crill, B. P., Werner, M., Akeson, R., et al. 2020, in Society of Photo-Optical Instrumentation Engineers (SPIE) Conference Series, Vol. 11443, Space Telescopes and Instrumentation 2020: Optical, Infrared, and Millimeter Wave, ed. M. Lystrup & M. D. Perrin, 114430I, doi: [10.1117/12.2567224](https://doi.org/10.1117/12.2567224)
- Darnley, M. J., Hounsell, R., O'Brien, T. J., et al. 2019, Nature, 565, 460, doi: [10.1038/s41586-018-0825-4](https://doi.org/10.1038/s41586-018-0825-4)
- Derdzinski, A. M., Metzger, B. D., & Lazzati, D. 2017, MNRAS, 469, 1314, doi: [10.1093/mnras/stx829](https://doi.org/10.1093/mnras/stx829)
- Dougherty, S. M., Waters, L. B. F. M., Bode, M. F., et al. 1996, A&A, 306, 547
- Fransson, C., Lundqvist, P., & Chevalier, R. A. 1996, ApJ, 461, 993, doi: [10.1086/177119](https://doi.org/10.1086/177119)
- Gatley, I., & Zuckerman, B. 1986, in Bulletin of the American Astronomical Society, Vol. 18, 1054
- Gatley, I., Hasegawa, T., Suzuki, H., et al. 1987, ApJL, 318, L73, doi: [10.1086/184940](https://doi.org/10.1086/184940)
- Harvey, E., Redman, M. P., Boumis, P., & Akras, S. 2016, A&A, 595, A64, doi: [10.1051/0004-6361/201628132](https://doi.org/10.1051/0004-6361/201628132)
- Healy-Kalesh, M. W., Darnley, M. J., Shara, M. M., et al. 2024, MNRAS, 529, 236, doi: [10.1093/mnras/stad3190](https://doi.org/10.1093/mnras/stad3190)
- Hessman, F. V. 1989, MNRAS, 239, 759, doi: [10.1093/mnras/239.3.759](https://doi.org/10.1093/mnras/239.3.759)
- José, J., & Hernanz, M. 1998, ApJ, 494, 680, doi: [10.1086/305244](https://doi.org/10.1086/305244)
- Kamiński, T., Mazurek, H. J., Menten, K. M., & Tyłenda, R. 2022, A&A, 659, A109, doi: [10.1051/0004-6361/202142737](https://doi.org/10.1051/0004-6361/202142737)

² <https://deepskycollective.com/home>

- Kastner, J. H., Weintraub, D. A., Gatley, I., Merrill, K. M., & Probst, R. G. 1996, *ApJ*, 462, 777, doi: [10.1086/177192](https://doi.org/10.1086/177192)
- Liimets, T., Corradi, R. L. M., Santander-García, M., et al. 2012, *ApJ*, 761, 34, doi: [10.1088/0004-637X/761/1/34](https://doi.org/10.1088/0004-637X/761/1/34)
- Miller Bertolami, M. M. 2016, *A&A*, 588, A25, doi: [10.1051/0004-6361/201526577](https://doi.org/10.1051/0004-6361/201526577)
- Morales-Rueda, L., Still, M. D., Roche, P., Wood, J. H., & Lockley, J. J. 2002, *MNRAS*, 329, 597, doi: [10.1046/j.1365-8711.2002.05013.x](https://doi.org/10.1046/j.1365-8711.2002.05013.x)
- Neugebauer, G., Habing, H. J., van Duinen, R., et al. 1984, *ApJL*, 278, L1, doi: [10.1086/184209](https://doi.org/10.1086/184209)
- Parsons, S. G., Rebassa-Mansergas, A., Schreiber, M. R., et al. 2016, *MNRAS*, 463, 2125, doi: [10.1093/mnras/stw2143](https://doi.org/10.1093/mnras/stw2143)
- Phillips, J. P., & Pottasch, S. R. 1984, *A&A*, 130, 91
- Ramos-Larios, G., Guerrero, M. A., Sabin, L., & Santamaría, E. 2017, *MNRAS*, 470, 3707, doi: [10.1093/mnras/stx1519](https://doi.org/10.1093/mnras/stx1519)
- Ritchey, G. W. 1901a, *ApJ*, 14, 167, doi: [10.1086/140849](https://doi.org/10.1086/140849)
- Ritchey, G. W. 1901b, *ApJ*, 14, 293, doi: [10.1086/140868](https://doi.org/10.1086/140868)
- Ritchey, G. W. 1902, *ApJ*, 15, 129, doi: [10.1086/140896](https://doi.org/10.1086/140896)
- Schember, H. R., Kemp, J. C., Ames, H. O., et al. 1996, in *Society of Photo-Optical Instrumentation Engineers (SPIE) Conference Series*, Vol. 2744, *Infrared Technology and Applications XXII*, ed. B. F. Andresen & M. S. Scholl, 751–760, doi: [10.1117/12.243518](https://doi.org/10.1117/12.243518)
- Scott, A. D., Rawlings, J. M. C., & Evans, A. 1994, *MNRAS*, 269, 707, doi: [10.1093/mnras/269.3.707](https://doi.org/10.1093/mnras/269.3.707)
- Seaquist, E. R., Bode, M. F., Frail, D. A., et al. 1989, *ApJ*, 344, 805, doi: [10.1086/167846](https://doi.org/10.1086/167846)
- Shara, M. M., Zurek, D., De Marco, O., et al. 2012, *AJ*, 143, 143, doi: [10.1088/0004-6256/143/6/143](https://doi.org/10.1088/0004-6256/143/6/143)
- Shara, M. M., Lanzetta, K. M., Garland, J. T., et al. 2024a, *MNRAS*, 529, 224, doi: [10.1093/mnras/stad3612](https://doi.org/10.1093/mnras/stad3612)
- Shara, M. M., Lanzetta, K. M., Masegian, A., et al. 2024b, *ApJL*, 977, L48, doi: [10.3847/2041-8213/ad991e](https://doi.org/10.3847/2041-8213/ad991e)
- Shara, M. M., Lanzetta, K. M., Masegian, A., et al. 2025, *AJ*, 170, 56, doi: [10.3847/1538-3881/addb44](https://doi.org/10.3847/1538-3881/addb44)
- Slavin, A. J., O’Brien, T. J., & Dunlop, J. S. 1995, *MNRAS*, 276, 353, doi: [10.1093/mnras/276.2.353](https://doi.org/10.1093/mnras/276.2.353)
- Speck, A. K., Meixner, M., Jacoby, G. H., & Knezek, P. M. 2003, *PASP*, 115, 170, doi: [10.1086/345911](https://doi.org/10.1086/345911)
- Starrfield, S., Bose, M., Iliadis, C., et al. 2024, *ApJ*, 962, 191, doi: [10.3847/1538-4357/ad1836](https://doi.org/10.3847/1538-4357/ad1836)
- Starrfield, S., Bose, M., Woodward, C. E., et al. 2025, *ApJ*, 982, 89, doi: [10.3847/1538-4357/adb8ed](https://doi.org/10.3847/1538-4357/adb8ed)
- Tweedy, R. W. 1995, *ApJ*, 438, 917, doi: [10.1086/175133](https://doi.org/10.1086/175133)
- Ventura, P., Tosi, S., García-Hernández, D. A., et al. 2025, *A&A*, 694, A177, doi: [10.1051/0004-6361/202452188](https://doi.org/10.1051/0004-6361/202452188)
- Weidmann, W. A., Mari, M. B., Schmidt, E. O., et al. 2020, *A&A*, 640, A10, doi: [10.1051/0004-6361/202037998](https://doi.org/10.1051/0004-6361/202037998)
- Werner, K., Reindl, N., Löbbling, L., et al. 2020, *A&A*, 642, A228, doi: [10.1051/0004-6361/202038574](https://doi.org/10.1051/0004-6361/202038574)